Biomineralization

DOI: 10.1002/anie.200700927

Intracellular Magnetite Biomineralization in Bacteria Proceeds by a Distinct Pathway Involving Membrane-Bound Ferritin and an Iron(II) Species**

*Damien Faivre, Lars H. Böttger, Berthold F. Matzanke, and Dirk Schüler**

Magnetotactic bacteria (MTB) are microorganisms that have the ability to navigate along geomagnetic field lines owing to the presence of magnetosomes, which are intracellular organelles comprising membrane-enveloped crystals of a magnetic material.[1] The unique crystalline and magnetic properties of magnetosomes have brought them into the focus of multidisciplinary interest as they are used in biotechnological applications[2] or as biomarkers for life on Mars.[3] Under microoxic conditions, the magnetotactic bacterium *Magnetospirillum gryphiswaldense* biomineralizes up to 100 cubooctahedral magnetite (Fe_3O_4) crystals per cell, which is accompanied by the intracellular accumulation of tremendous amounts of iron (up to 4% of the dry weight[4]). This amount indicates that MTB use very efficient systems for uptake, transport, and precipitation of iron that, however, are still poorly understood. On the basis of Mössbauer spectroscopic and biochemical analyses, it was suggested that for bacterial magnetite formation, Fe^{3+} ions are taken up from the environment and subsequently reduced intracellularly. Mineral precipitation then occurs within the magnetosome vesicles, possibly by partial reduction of a hydrated ferric oxide.[5–7]

However, individual steps of the mechanism have remained obscure, as previous approaches were limited owing to an insufficient control of growth rate and extracellular oxygen concentrations during bacterial cultivation. In particular, no time-resolved data from early steps of magnetite precipitation are available. Thus, the following questions are addressed in this study:

1) Which iron species are transported from the cell exterior into the magnetosome vesicles?
2) Are there any inorganic phases in addition to magnetite associated with magnetosomes, for example, a precursor such as ferrihydrite ($Fe_5HO_8{\cdot}4H_2O$) or an oxidized phase such as maghemite (γ-Fe_2O_3)?
3) Are the metabolic routes of intracellular iron used for the biosynthesis of magnetite the same as those involved in general iron metabolism in nonmagnetic cells?

In this study, we used a cell-suspension assay for the growth-independent study of magnetite formation under highly controlled conditions. Mössbauer spectroscopy and electron microscopy were employed for time-resolved analysis of the intracellular iron metabolite pattern of iron-induced magnetosome formation.

Magnetite formation could be induced in iron-starved nonmagnetic wild-type (WT) cells by the addition of either ferric citrate or ferrous ascorbate (Figure 1), indicating that the bacteria are capable of intracellular reduction or oxidation of extracellular iron to form the mixed-valence Fe_3O_4 crystals. Magnetite crystallites were not detected by TEM until 55 min after iron addition, coincident with the appearance of magnetically oriented cells as detected by C_{mag} measurements (Figure 1). Over time, the average particle dimensions increased from 18.1 to 31.5 nm, and the number of crystals per cell from 16 to 30. After 6 h, formation of chains was complete. Electron diffraction (ED) revealed that magnetosome particles at all stages consisted exclusively of magnetite, as no other mineral phase or structure could be detected (data not shown), although ferrihydrite might have escaped detection by ED owing to its poor crystallinity.[8]

In Figure 2a, typical Mössbauer spectra of whole cells, 20 h after induction and at 130 K (spectrum A) and 4.3 K (spectrum B), are presented; the corresponding Mössbauer parameters are listed in Table 1. Mössbauer spectra can be characterized by three different parameters: the isomer shift δ, the quadrupole splitting ΔE_Q, and the magnetic hyperfine field B_{HF}. In the absence of quadrupole splitting or magnetic

[*] Prof. D. Schüler
Microbiology
Department of Biology
LMU München
Maria-Ward-Strasse 1a, 80638 München (Germany)
Fax: (+49) 89-2180-6127
E-mail: dirk.schueler@lrz.uni-muenchen.de
Dr. D. Faivre,[+] Prof. D. Schüler
Department of Microbiology
Max Planck Institute for Marine Microbiology
Celsiusstrasse 1, 28359 Bremen (Germany)
L. H. Böttger
Institute of Physics
University of Lübeck
Ratzeburger Allee 160, 23538 Lübeck (Germany)
Prof. B. F. Matzanke
Isotopes Laboratory
University of Lübeck
Ratzeburger Allee 160, 23538 Lübeck (Germany)
[+] Current address:
Max-Plank-Institut für Kolloid- und Grenzflächenforschung
Abteilung Biomaterialien
Wissenschaftspark Golm, 14424 Potsdam (Germany)

[**] This research was supported by the Max Planck Society and the Biofuture program of the BMBF. R. Sonntag is acknowledged for help with the fermentation procedure and J. Schorch for technical assistance with the cell fractioning. D.F. acknowledges support from a Marie Curie Fellowship from the European Union (project BacMag, EIF-2005-009637).

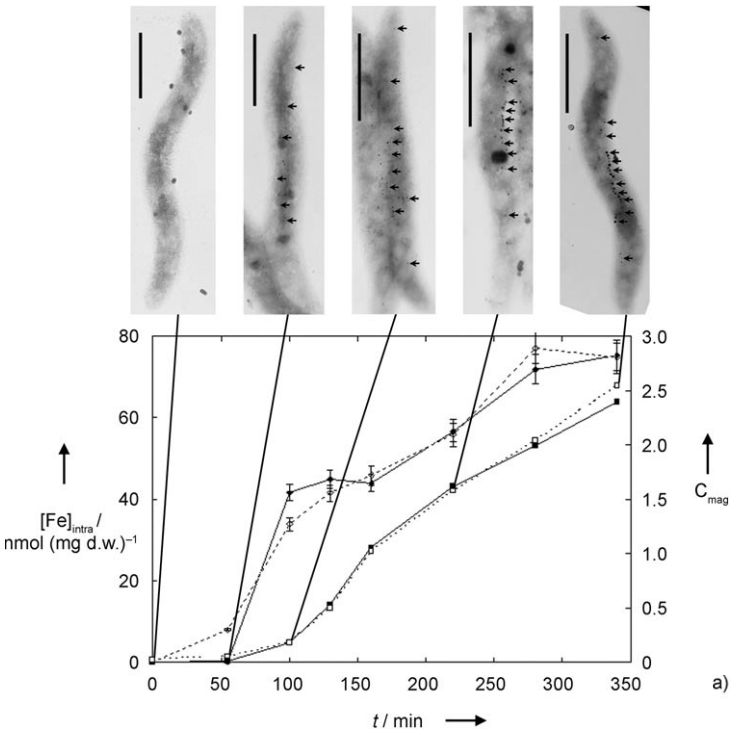

Figure 1. Time-resolved magnetosome formation after induction: Magnetite formation was induced in resting iron-deprived cells by addition of either Fe^{II} or Fe^{III} into the medium (black symbols and continuous line for Fe^{III}, open symbols and dashed line for Fe^{II}) and was followed by intracellular iron accumulation ($[Fe]_{intra}$ (d.w.: dry weight), diamonds), magnetic response (C_{mag}, squares), and TEM. The micrographs show the increase in particle number and dimensions (arrow pointed at every third magnetosome) in representative cells at different times after induction (scale bar: 1 μm). Formation of chains is complete after 340 minutes.

interaction, a single resonance absorption is observed, which is characterized by the isomer shift δ. It originates from the electric monopole interaction between the nucleus and electronic shell. The isomer shift is a measure for the oxidation state and for the degree of covalent bonding of the iron atom with the ligand. The quadrupole splitting ΔE_Q originates from the electric quadrupole interaction between the nucleus and electronic shell. It results in the splitting of the resonance absorption line and is a measure for the symmetry of the metal chelate and for the covalent distribution of ligand–metal bonding. Finally, the magnetic hyperfine field B_{HF} is a result of magnetic dipole interaction between the nucleus and electrons and generates six-line or even more complicated spectra.

In our experiments, the spectrum at 130 K exhibits two magnetically split sextets attributed to magnetite A and B sites (subspectrum 1 and 2, respectively, in Figure 2a),[5,9,10] high-spin $[Fe^{2+}(O/N)_6^{x-}]^{2-x}$ (subspectrum 3 in Figure 2a, oxygen or oxygen/nitrogen ligands), and an Fe^{3+} quadrupole doublet (subspectrum 4 in Figure 2a). The Fe^{3+} doublet species displays features typical of ferrihydrite ($(FeOOH)_8 \cdot (FeOH_2PO_4)$) and not of FeOOH.[9,11]

The biogenic origin of this material, that is, ferritin and not inorganic ferrihydrite, was further verified by biochemical analysis. In SDS-PAGE (sodium dodecylsulfate polyacrylamide gel electrophoresis) of the membrane and soluble fractions of disrupted cells, a reddish, high-molecular-mass protein ($M > 100$ kDa) that carries large amounts of iron and disintegrates into 20–40-kDa subunits (data not shown) could be identified. The spectrum at 4.3 K is dominated by a typical magnetite six-line pattern. The ferrihydrite doublet seen in the spectrum at 130 K is completely missing at 4.3 K as a result of magnetic ordering. The six-line pattern of ferrihydrite is, however, not visible as a distinct species at 4.3 K because it is masked by the dominant magnetite and will only exhibit very broad lines caused by the typical particle distribution of ferritin. The magnetic transition above 4.3 K indicates that either the magnetic anisotropy constant K or the volume V of the crystallites is larger than in typical bacterial ferritins,[11] a feature which fits better with mammalian-type ferritin exhibiting a low phosphate contribution.

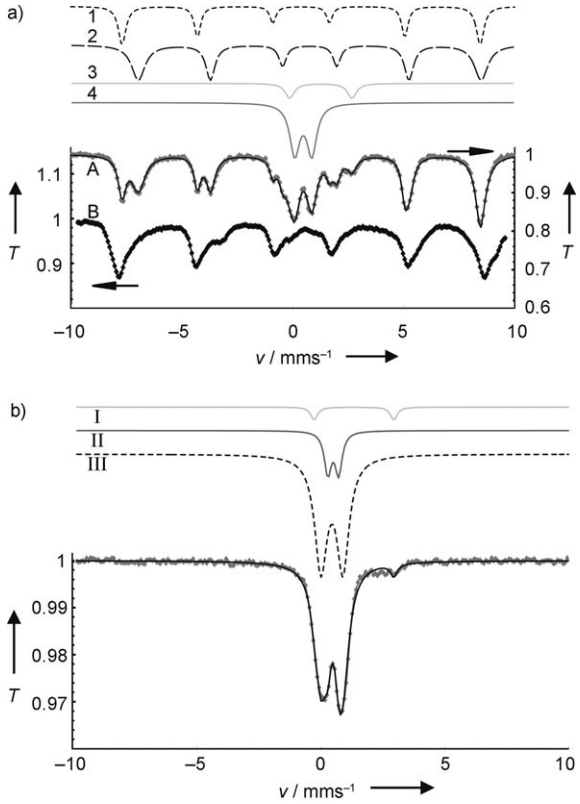

Figure 2. a) Mössbauer spectrum of whole WT cells after 1230 min of magnetite formation at 130 K (A) and 4.3 K (B). The spectrum at 130 K consists of two magnetite sextets (1 and 2), an Fe^{2+} component (3), and a ferritin doublet (4); individual components are represented by dashed or faded traces, with the addition of the components shown with ——. At 4.3 K the ferritin doublet vanishes and forms a magnetically split sextet beneath the magnetite components, which are broadened owing to their Verwey transition. The transmission T is scaled to 1. b) Mössbauer spectra of the mutant strain MSR-1B at 80 K. Jagged gray trace: experimental data; ——: addition of the individual components; III) ferritin; I) Fe^{II}; II) unspecified iron component.

Table 1: Summary of the Mössbauer parameters used to fit the spectra. The numbers in parentheses correspond to the subspectra.

Sample	T [K]	δ [mms^{-1}]	ΔE_q [mms^{-1}]	B_{HF} [T]	Relative contribution [%]
Whole cells					
magnetite A (1)	130	0.38	0	49.5	23.9
magnetite B (2)	130	0.76	0	47.4	47.8
Fe^{II} (3)	130	1.27	2.81	–	6.4
ferritin (4)	130	0.47	0.77	–	21.9
IM					
magnetite A (5)	130	0.38	0	49.9	33.3
magnetite B (6)	130	0.76	0	47.9	66.7
SF					
ferritin[a] (7)	4.3	0.49	0.77	–	13.2
ferritin[b] (8)	4.3	0.49	0	47.4	86.8
ferritin (9)	77	0.47	0.77	–	100
MF					
small magnetite A (10)	130	0.38	0	46.8	4.3
small magnetite B (11)	130	0.76	0	44.8	8.6
Fe^{II} (12)	130	1.26	2.86	–	9.0
ferritin (13)	130	0.47	0.77	–	78.1

[a] Relaxing part. [b] Nonrelaxing part, hyperfine distribution.

All Mössbauer spectra of whole WT cells of the induction experiments exhibit the same components as the Mössbauer spectra of Figure 2a. By Mössbauer spectroscopy, first traces of magnetite, ferritin, and Fe^{2+} were detected already 20 minutes after induction with $^{57}Fe^{3+}$ citrate (Figure 3a,b). The amount of all components increases within 40 min. Then, the Fe^{2+} and ferritin contributions only slightly change whereas magnetite growth accelerates. The magnetite growth rate decelerates 215 min after induction (Figure 3b).

As expected, no magnetite was detected by TEM and Mössbauer spectroscopy in mutant strain MSR-1B, which lacks the magnetosome genes as a result of deletion. Mutant cells (Figure 2b) were also shown to contain: an Fe^{2+} species (subspectrum I in Figure 2b), which however was present in lower quantities than in the WT; an unspecified compound (subspectrum II in Figure 2b), which might possibly be an iron–sulfur protein; and ferritin (subspectrum III in Figure 2b). This observation suggests that two different metabolic routes for the intracellular iron might coexist, one to satisfy biochemical requirements comprising ferritin and small amounts of Fe^{2+}, and the other one comprising Fe^{2+} and magnetite. Experiments involving shifts of iron-replete, but nonmagnetic, cells to iron-depleted conditions indicated that these pools are not readily interchangeable in the WT (data not shown).

Nonmagnetic soluble fraction (SF) and membrane fraction (MF) and the isolated magnetic magnetosomes (IMs) were separated from disrupted mature cells with fully developed magnetosome chains to determine the subcellular localization of the observed iron species. The IMs exclusively exhibited the typical two sextets (subspectra 5 and 6 in Figure 4a) of magnetite. This result was unexpected, as a magnetic sextet compound was identified by Mössbauer spectroscopy in magnetosome preparations from the closely related *M. magnetotacticum* and attributed to ferrihydrite.[6] On the basis of this observation, after uptake and partial oxidation of Fe^{2+}, the following mechanism including ferrihydrite as a precursor was proposed [Eqs. (1), (2)].

$$5\,Fe^{3+} + 5\,H_2O \rightarrow 5\,Fe(OH)_x^{3-x} \\ +5\,H^+ \rightarrow Fe_5HO_8 \cdot 4\,H_2O \quad (1)$$

$$Fe_5HO_8 \cdot 4\,H_2O + Fe^{2+} \rightarrow Fe_3O_4 \quad (2)$$

In our study, the MF and SF (Figure 4b,c) yielded spectra consistent with ferritin (subspectra 7–9, 13 in Figure 4b,c), an Fe^{2+} compound (subspectrum 12 in Figure 4c), and a conspicuous compound present in low amount (subspectra 10 and 11 in Figure 4c). Fe^{2+} species, similar to that observed in *M. gryphiswaldense*, have been detected in many bacterial systems and were attributed to a cytoplasmic low-molecular-mass Fe^{2+} pool.[12] Surprisingly, the Fe^{2+} ions found here were predominantly present in the MF, whereas only little Fe^{2+} was observed in the SF. The

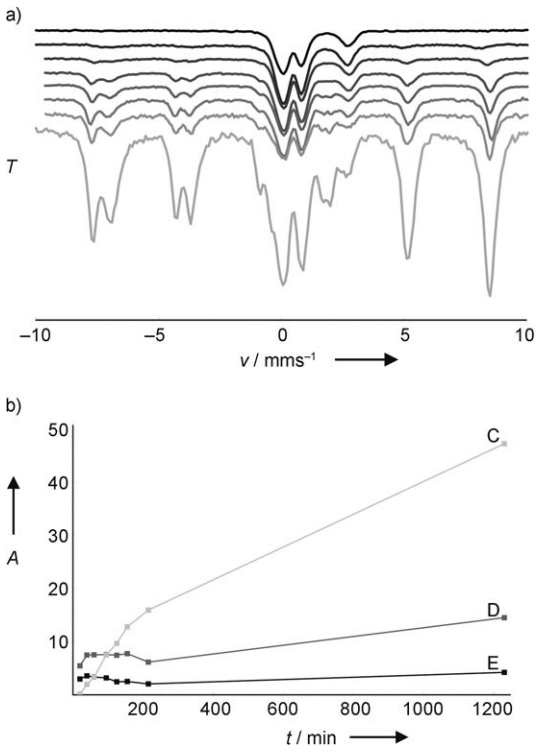

Figure 3. a) Stack graph of the Mössbauer spectra at different times after iron induction. From top (black) to bottom (light gray): 20, 40, 60, 95, 125, 155, 215, and 1230 min after ^{57}Fe induction. b) Total areas *A* of the Mössbauer spectra (scaled by sample masses) plotted against time after ^{57}Fe induction: high-spin Fe^{II} (black, E), ferritin (dark gray, D), and magnetite (A and B sites; light gray, C). The lines are shown only as a guide for the eyes.

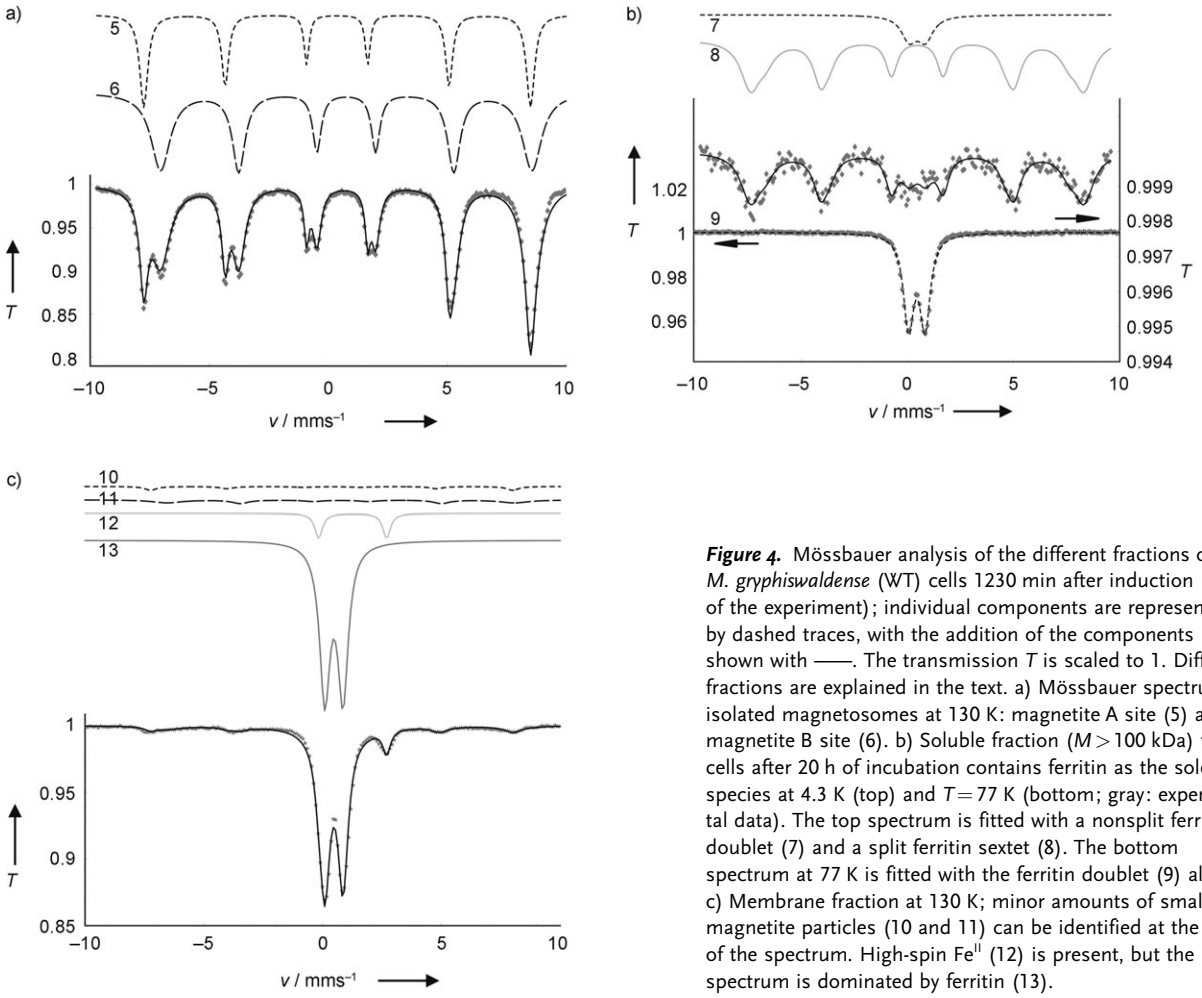

Figure 4. Mössbauer analysis of the different fractions of the *M. gryphiswaldense* (WT) cells 1230 min after induction (end of the experiment); individual components are represented by dashed traces, with the addition of the components shown with ——. The transmission *T* is scaled to 1. Different fractions are explained in the text. a) Mössbauer spectrum of isolated magnetosomes at 130 K: magnetite A site (5) and magnetite B site (6). b) Soluble fraction ($M > 100$ kDa) from cells after 20 h of incubation contains ferritin as the sole iron species at 4.3 K (top) and $T = 77$ K (bottom; gray: experimental data). The top spectrum is fitted with a nonsplit ferritin doublet (7) and a split ferritin sextet (8). The bottom spectrum at 77 K is fitted with the ferritin doublet (9) alone. c) Membrane fraction at 130 K; minor amounts of small magnetite particles (10 and 11) can be identified at the flanks of the spectrum. High-spin Fe^{II} (12) is present, but the spectrum is dominated by ferritin (13).

ferritin-type component, whose nature was further proven by SDS- and native-PAGE (Fridovich staining) in both the SF and the MF of disintegrated cells,[20] exhibits a superparamagnetic transition below 77 K (subspectra 7 and 8 at 4.3 K and spectrum 9 at 77 K in Figure 4b). The splitting and line shape of the conspicuous compound are consistent with very small magnetite particles (< 5 nm)[10] because the signal is magnetically split above 120 K but exhibits a magnetic hyperfine field of merely 44–45 T. This signal is most likely obscured in the spectra of whole cells by the strong signal of large magnetite crystals in the magnetosomes.

Our data suggest the following pathway of magnetite biomineralization (Figure 5): Iron is taken up from the environment either as Fe^{2+} or Fe^{3+} and is converted into an intracellular ferrous high-spin species predominantly located in the membrane and into a membrane-associated ferritin. As we were unable to detect a putative mineral precursor, magnetite precipitation has to proceed during the subsequent steps by fast coprecipitation of Fe^{2+} and Fe^{3+} ions within the magnetosome compartment. This compartment is likely alkaline, thus enabling thermodynamic stability of magnetite [Eqs. (3), (4)].[13]

$$Fe^{2+}A + 2\,Fe^{3+}B + (x+y)\,H_2O \rightarrow 2\,Fe(OH)_x^{3-x} + Fe(OH)_y^{2-y} + (x+y)H^+ + A^{2-} + B^{3-} \quad (3)$$

$$2\,Fe(OH)_x^{3-x} + Fe(OH)_y^{2-y} \rightarrow Fe_3O_4\ (\text{crystal in statu nascendi}) + (2x+y-4)\,H_2O \quad (4)$$

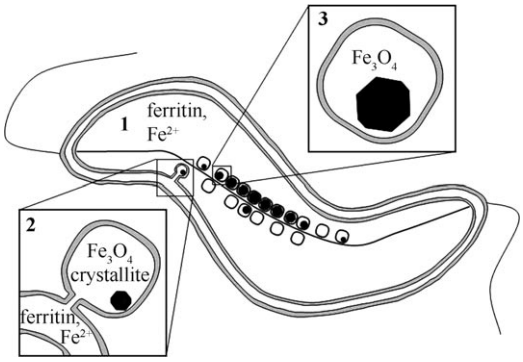

Figure 5. Model of iron uptake and magnetite formation mechanism. A biochemical pool of iron is formed in the cells, essentially composed of ferritin and Fe^{2+} (**1**). Magnetite biomineralization proceeds first by transport of Fe^{2+} ions and ferritin into invaginated magnetosome vesicles where Fe^{2+} and Fe^{3+} ions coprecipitate (**2**). Final magnetite growth then occurs in fully formed mature magnetosomes (**3**).

At the cytoplasmic membrane (CM) level the Fe^{2+} and Fe^{3+} ions are ligated by organic substrates (A: structure unknown; B: ferritin) and are released at the magnetosome–compartment interface. However, Fenton chemistry and thermodyamic properties preclude the presence of hexaquo or hydroxo complexes in the membrane. A recent study of *M. magneticum* has shown that the magnetosome membrane (MM) originates from the CM by invagination, and these compartments are at least transiently contiguous,[14] which is consistent with our observation by Mössbauer spectroscopy of small magnetite particles associated with the membrane. On the other hand, biochemical and ultrastructural data in the closely related *M. gryphiswaldense* suggest that during later development MM vesicles become detached from the CM and form a distinct compartment after differentiation.[15,16] According to these observations, a process has to be assumed, by which nucleation of magnetite crystallites predominantly occurs at the CM level and the subsequent growth happens after mature iron-loaded vesicles are separated from the CM.

In summary, we propose a mechanism for magnetite formation, by which iron required for magnetite biomineralization is processed throughout cell membranes directly to the MM without iron transport through the cytoplasm, suggesting that pathways for magnetite formation and biochemical iron uptake are distinct. Magnetite formation occurs via membrane-associated crystallites, whereas the final step of magnetite crystal growth possibly is spatially separated from the CM.

Experimental Section

The *Magnetospirillum gryphiswaldense* strain MSR-1 (DSMZ 6361) and nonmagnetic mutant strain MSR-1B[17] were used throughout all experiments. Cells were grown in bioreactors using a modified protocol for large-scale cultivation of *M. gryphiswaldense* under defined conditions.[18] Inductions were performed with enriched ^{57}Fe as $^{57}Fe^{3+}$ citrate ($C_6H_5FeO_7 \cdot x\,H_2O$; $x = 2$—3) to achieve a higher effect and a better resolution for the analysis of the Mössbauer spectra. The average magnetic orientation (C_{mag}) of cell suspensions was assayed by an optical method.[19] For growth-independent induction experiments, cells that were in the midlogarithmic growth phase were transferred to a low-carbon-content medium.[16] Under these conditions, no or weak cell growth occurred, but cells remained viable and kept the capability to biomineralize magnetosomes.

At specified time intervals, samples of 2.0 mL were withdrawn from the culture for C_{mag} determination and TEM analysis. Bright-field TEM images were obtained with a Zeiss EM10 transmission electron microscope at an accelerating voltage of 60 kV. Simultaneously, cell suspensions ranging from 1 to 2 L were centrifuged; the pellets were weighed, transferred to Delrin sample holders, and frozen in liquid nitrogen for later Mössbauer analysis. The Mössbauer spectrometer was operated in the constant acceleration mode. The spectrometer was calibrated against an α-iron foil at room temperature. The samples were kept for measurements in continuous flow and bath cryostats (Oxford). The spectra were analyzed by least-squares fits using Lorentzian line shapes. Spectra were recorded at a sample temperature of 130 K. Whole, mature cells and the ferritin-containing cell fractions were also measured at 77 K and 4.3 K.

Magnetosomes were separated by a previously developed methodology.[15] After removal of magnetosomes, residual cell fractions were further separated in a Beckman J-E high-velocity centrifuge (20 min at 16000 *g*; sediment). This step was skipped for the 20-h sample. Ultracentrifugation of the supernatant was performed in a Beckman Optima Max E at 100.000 *g* for 1 h. The washed pellet, which was considered to represent the membrane fraction (MF), and the supernatant (SF) were analyzed to determine the iron and protein content.

Received: March 1, 2007
Revised: May 30, 2007
Published online: September 27, 2007

Keywords: biomineralization · magnetic properties · magnetotactic bacteria · Mössbauer spectroscopy · reaction mechanisms

[1] D. A. Bazylinski, R. B. Frankel, *Nat. Rev. Microbiol.* **2004**, *2*, 217.
[2] C. Lang, D. Schüler, D. Faivre, *Macromol. Biosci.* **2007**, *7*, 144.
[3] D. S. McKay, E. K. Gibson Jr. , K. L. Thomas-Keprta, H. Vali, C. S. Romanek, S. J. Clemett, X. D. F. Chilier, C. R. Maechling, R. N. Zare, *Science* **1996**, *273*, 924.
[4] D. Schüler, E. Baeuerlein, *J. Bacteriol.* **1998**, *180*, 159.
[5] R. B. Frankel, R. Blakemore, R. S. Wolfe, *Science* **1979**, *203*, 1355.
[6] R. B. Frankel, G. C. Papaefthymiou, R. P. Blakemore, W. O'Brien, *Biochim. Biophys. Acta Mol. Cell Res.* **1983**, *763*, 147.
[7] D. Schüler, E. Baeuerlein, *Arch. Microbiol.* **1996**, *166*, 301.
[8] S. Mann, R. B. Frankel, R. P. Blakemore, *Nature* **1984**, *310*, 405.
[9] R. M. Cornell, U. Schwertmann, *The Iron Oxides (Structure, Properties, Reactions, Occurrences and Uses)*, Wiley-VCH, Weinheim, **2003**.
[10] S. Mørup, J. A. Dumesic, H. Topsøe, in *Magnetic Microcrystals, Vol. 11* (Ed.: R. L. Cohen), Academic Press, New York, **1980**, p. 1.
[11] B. F. Matzanke, in *Transition Metals in Microbial Metabolism* (Eds.: G. Winklemann, C. Carrano), Harwood academic publishers, Amsterdam, **1997**, p. 117.
[12] R. Böhnke, B. F. Matzanke, *BioMetals* **1995**, *8*, 223.
[13] D. Schüler, *Magnetoreception and Magnetosomes in Bacteria*, *Vol. 3*, Springer, Heidelberg, **2006**.
[14] A. Komeili, Z. Li, D. K. Newman, G. J. Jensen, *Science* **2006**, *311*, 242.
[15] K. Grünberg, E. C. Müller, A. Otto, R. Reszka, D. Linder, M. Kube, R. Reinhardt, D. Schüler, *Appl. Environ. Microbiol.* **2004**, *70*, 1040.
[16] A. Scheffel, M. Gruska, D. Faivre, A. Linaroudis, J. M. Plitzko, D. Schüler, *Nature* **2006**, *440*, 110.
[17] S. Schübbe, M. Kube, A. Scheffel, C. Wawer, U. Heyen, A. Meyerdierks, M. Madkour, F. Mayer, R. Reinhardt, D. Schüler, *J. Bacteriol.* **2003**, *185*, 5779.
[18] U. Heyen, D. Schüler, *Appl. Microbiol. Biotechnol.* **2003**, *61*, 536.
[19] D. Schüler, R. Uhl, E. Baeuerlein, *FEMS Microbiol. Lett.* **1995**, *132*, 139.
[20] Unpublished results.

